CIVIL AND ENVIRONMENTAL ENGINEERING REPORTS

E-ISSN 2450-8594

CEER 2026; 36 (4): 0064-0082
DOI: 10.59440/ceer/242093
Original Research Article

HYDRO-THERMAL PERFORMANCE AND EVAPORATIVE COOLING EFFICIENCY OF PERVIOUS CONCRETE PAVERS INCORPORATING RECYCLED SEASHELL AGGREGATES

Mohamed Lemine MOHAMED ESSALEM[1], Khaled SEIFEDDINE[2], Sofiane AMZIANE[2], Toufik CHERRADI[1], Mohamed Cheikh TEGUEDY[3*]
[1]University Mohammed V, Mohammadia School of Engineers, Rabat, Morocco
[2]CNRS, SIGMA Clermont, Institut Pascal, Université Clermont Auvergne, Clermont-Ferrand, France
[3]École Supérieure Polytechnique, Groupe Polytechnique, Nouakchott, Mauritania

Abstract

Pervious concrete pavements offer multifunctional urban benefits by mitigating stormwater runoff and providing evaporative surface cooling. Incorporating recycled aggregates into these systems further enhances sustainability by supporting circular-economy initiatives, through the recovery of seashells as construction aggregates and reduced demand for virgin mineral resources. This study investigates the influence of recycled seashell aggregates on pervious concrete pavers by comparing a baseline control formulation with a seashell-based mixture. A unified experimental framework was utilized to assess physical and mechanical properties, hydraulic performance, thermo-physical parameters, and surface thermal responses under controlled dry–wet testing with repeatable radiative forcing. The seashell-based formulation exhibited a 72% increase in open porosity and a 137% increase in measured infiltration rate, enhancing hydraulic functionality. This increase in open porosity was accompanied by a mechanical trade-off, reducing compressive strength to 4.44 MPa (38% of control), alongside a 43% decrease in thermal conductivity. During dry thermal testing, seashell pavers cooled faster at night (up to 5 °C lower). In wet testing, SPCP showed an average water-loss rate of 4.81 g/h over the first three days and daytime surface temperature reductions up to 7 °C and nighttime reductions up to 4 °C. Overall, recycled seashell aggregates enhance infiltration and evaporative cooling performance at the expense of structural capacity, supporting their potential for stormwater management and heat mitigation, subject to mechanical and durability validation for the intended application.

Keywords: pervious concrete pavers, seashell by-products, albedo, thermal conductivity, surface temperature

[*] Corresponding author: École Supérieure Polytechnique, Groupe Polytechnique, Nouakchott, Mauritania, e-mail: med_cheikh.teguedy@esp.mr, tel. +222 47 77 77 81

1. INTRODUCTION

Urban areas increasingly face two interconnected challenges: stormwater management during intense rainfall events and surface overheating associated with the urban heat island effect (UHI) [1]. Conventional dense pavements generate substantial runoff and store sensible heat, thereby aggravating peak flows, flood risk and outdoor thermal stress [2]. In this context, pervious concrete pavements (PCPs) are increasingly considered multifunctional infrastructure because they can enhance rainwater infiltration while contributing to surface-temperature regulation, particularly when moisture is available for evaporative cooling [3–7].

Despite these advantages, PCP performance is governed by a critical design trade-off: increasing the connected void content generally enhances surface infiltration and water storage but reduces mechanical strength and can affect durability and long-term hydraulic efficiency, particularly through clogging [3,8]. Consequently, contemporary research has changed from maximizing a single property to balancing structural capacity with hydraulic and thermal functions. However, paver cooling is not controlled by porosity alone. It results from interactions among radiative properties, particularly albedo; thermophysical properties, including thermal conductivity and heat-storage capacity; and moisture retention and transport. The relative importance of these processes differs markedly between the dry and wet states [2,9,10].

In parallel, the incorporation of recycled or waste-derived materials into cementitious composites has become an important pathway toward more resource-efficient construction by reducing the demand for virgin aggregates and creating value from residual material streams [11–13]. Recovered seashell waste generated by aquaculture and seafood-processing industries represents a potential alternative aggregate, particularly in coastal regions, due to its local availability and predominantly calcium-carbonate composition. Global shellfish production generates large quantities of discarded shells [14], and experimental studies have demonstrated the feasibility of using processed seashells as partial or complete replacements for conventional aggregates. Depending on their processing method and replacement level, seashell aggregates can increase porosity and water absorption, thereby modifying transport properties while generally reducing mechanical strength [13,15–18]. Recent reviews confirm these trends and highlight the potential of recovered seashell aggregate to modify the pore structure and transport behaviour of cementitious materials [19]. However, although seashells have already been investigated in conventional concrete and pervious concrete pavers, their influence on the combined pore structure, surface infiltration, and thermal response of pervious pavers under controlled dry and wet conditions remains insufficiently documented [15,16,20–22].

More specifically, direct comparisons of transient surface-temperature evolution under reproducible radiative conditions in both dry and wet states remain scarce. Therefore, controlled laboratory benches have been developed to investigate the surface-energy balance and thermal behaviour of permeable pavements under well-defined boundary conditions [8,9]. These systems allow surface temperature and radiative fluxes to be monitored during radiative heating and subsequent lamp-off cooling, while moisture-loss measurements can support the interpretation of evaporative cooling.

This study compares a control pervious concrete paver (CPCP) with a paver in which the natural coarse aggregate is completely replaced by recovered seashell aggregate (SPCP). It addresses three research questions: (i) how does this replacement modify the balance between open porosity, surface infiltration and compressive strength; (ii) how does it affect the surface temperature response under identical dry and wet radiative heating cycles; and (iii) does SPCP continue to release water beyond the first three days of drying, without any additional water supply? To answer them, the experimental programme combines physical and mechanical characterization (bulk density, water-accessible open

porosity and 28-day compressive strength), hydraulic and thermophysical measurements (surface infiltration rate, thermal conductivity and albedo), and transient surface-temperature monitoring under reproducible radiative forcing in dry and initially saturated states, together with the mass change of SPCP during drying.

Because the two aggregates differ in grading, particle shape, absorption and packing, their combined effect is hypothesized to increase infiltration and wet-state cooling at the cost of compressive strength. The novelty of this work lies in the joint assessment of hydraulic, mechanical and thermal responses within a single controlled dry–wet framework. As only two formulations are compared, the results are interpreted as formulation effects and do not identify an optimum seashell content.

2. EXPERIMENTAL PROGRAM

2.1. Raw materials

Portland-composite cement CEM II 32.5 was used as the binder for all pervious concrete mixtures. Two types of coarse aggregates were considered: conventional natural aggregates (NA) and seashell aggregates (SA) (Fig. 1). Natural aggregates with a particle size range of 4–12.5 mm were used for the control pervious concrete pavers (CPCP), while crushed seashell aggregates with a particle size range of 5–14 mm were used for the seashell-based pervious concrete pavers (SPCP). The particle size distributions used are shown in Fig. 2.

The seashells were obtained from the Akreidil seashell accumulations in Mauritania through a local supplier, after crushing and screening, thoroughly washed to remove organic impurities, oven-dried at 105 °C for 6 h and sieved to obtain the desired size fraction. The mineralogical composition of the seashell aggregates was characterized by X-ray diffraction (XRD) (see Fig. 3), confirming that calcium carbonate in the aragonite phase was the dominant constituent, in agreement with previous studies on seashell-based aggregates [17,20,23].

The physical properties of the aggregates, including bulk density, specific gravity, water absorption and Los Angeles abrasion coefficient, were determined according to relevant ASTM standards. Water absorption was measured after 24 h according to ASTM C127 [25].

The aggregate properties are listed in Table 1. As reported in previous works, seashell aggregates exhibited significantly lower bulk density and higher water absorption compared to natural aggregates, which is expected to influence the pore structure, hydraulic behaviour and thermal response of the resulting pervious concrete [16,24].



Fig. 1. Natural and seashell aggregates

Table 1. The properties of aggregates

Properties	NA	SA
Bulk density (kg/m³) — ASTM C29 [26]	1620	760
Specific gravity — ASTM C127-15 [25]	2.757	2.860
Water absorption at 24 h (%) ASTM C127-15 [25]	0.55	3.46
Los Angeles coefficient (%)	15	23.84

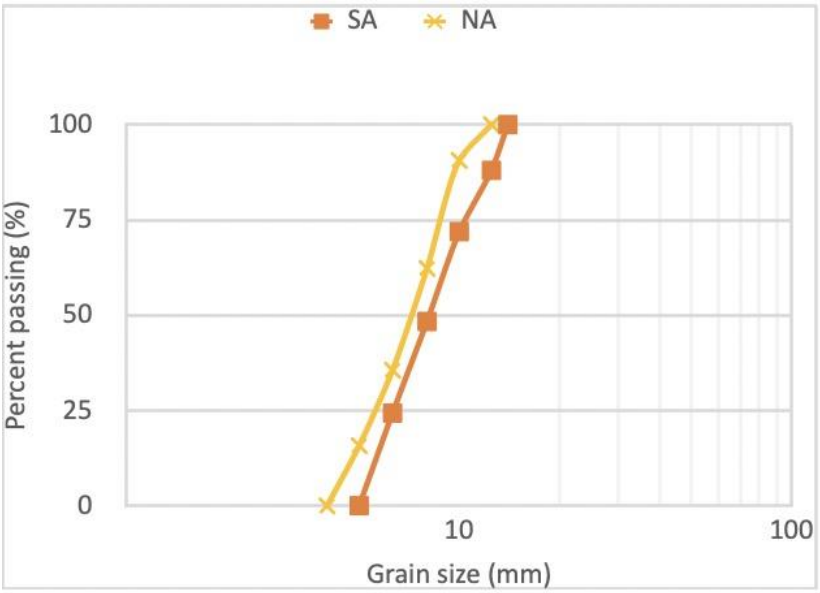

Fig. 2. Granulometric analysis of aggregates

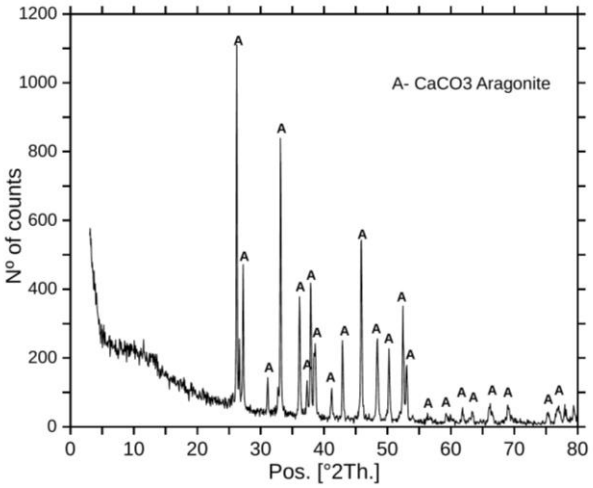

Fig. 3. XRD pattern of seashell

2.2. Mix design and specimen preparation

Two pervious concrete mixtures were prepared: a control mixture using natural aggregates (CPCP) and a seashell-based mixture using seashell aggregates as a full replacement of natural coarse aggregates (SPCP). The mix proportions were kept identical for both mixtures in terms of cement content, aggregate content and water-to-cement ratio in order to assess the combined effect of replacing the aggregate on the physical, hydraulic and thermal behaviour of the pavers.

The cement content was fixed at 350 kg/m³, the aggregate content at 1600 kg/m³ and the water-to-cement ratio at 0.32 (Table 2), in accordance with typical mixture designs for pervious concrete pavements reported in the literature [27–29]. Mixing was performed in a pan mixer to ensure homogeneous distribution of cement paste around the aggregates while preserving the interconnected pore structure characteristic of pervious concrete. Both aggregate types were dry at mixing, and no additional water was supplied to compensate for absorption. The nominal water-to-cement ratio was therefore the same, but the water available to the paste could differ between mixtures.

After casting, the specimens were compacted in three layers by vibration without applied pressure to avoid excessive paste flow and pore clogging. All specimens were demoulded after 24 h and cured under controlled laboratory conditions until testing at 28 days. Three types of specimens were prepared: cylindrical specimens (11 cm × 22 cm) for density, porosity and compressive strength tests; parallelepiped specimens (15 × 15 × 6 cm³) for thermal conductivity measurements; and large slabs (30 × 40 × 5 cm³) for infiltration and thermal behaviour tests (Fig. 4).

Table 2. Mixture proportions

Specimens	Gravel (kg/m³)	Cement (kg/m³)	Water (kg/m³)	W/C
CPCP	1600	350	112	0.32
SPCP	1600	350	112	0.32



Fig. 4. Prepared samples

2.3. Physical and mechanical characterization

2.3.1. Bulk density and open porosity

Bulk density was determined from dry mass and specimen volume. Open porosity was measured by filling the accessible voids with water, following the method described by Seifeddine et al. [8]. Prior to testing, specimens were oven-dried at 40 °C until constant mass to avoid microstructural damage. The specimen was placed in a rigid mould sealed with PVC film. The mould and specimen were weighed before and after water was added to fill the accessible voids; their mass difference gave the volume of added water. The open porosity was determined using Eq. (2.1) [8,30,31].

This method provides an estimate of the water-accessible void volume, which is a key parameter governing both hydraulic performance and evaporative cooling potential of pervious pavements [32]. Pore connectivity and pore-size distribution were not measured independently.

$$Po = [(Ms - Ma) / (\rho e \cdot Vt)] \times 100\ \% \quad (2.1)$$

Po: open or effective porosity, [%],
Ma: mass of the mould and dry specimen before water filling, [kg],
Ms: mass of the mould and specimen after water filling, [kg],
Vt: total volume of the sample, [m³],
ρe: water density, [kg·m^{-3}]. The same mould was included in both mass readings, so its mass cancels in the difference.

2.3.2. Compressive strength

Compressive strength tests were performed at 28 days on cylindrical specimens in accordance with EN 12390-3, with three specimens per formulation. The compressive strength results were used to compare the mechanical capacity of the two formulations and discuss potential low-traffic applications, in line with previous studies on pervious and lightweight concrete pavements [14,29].

2.4. Hydraulic characterization

Surface infiltration was measured by recording the time required for a known quantity of water to drain completely from a column through the specimen surface. Three measurements were repeated on one slab per formulation. The measured infiltration rate was calculated using the mass–area–time expression in ASTM C1701/C1701M [33], given in Eq. (2.2). The water head decreased during drainage; this laboratory procedure is therefore described explicitly rather than as a standard falling-head permeability test.

$$I = \gamma M / (D^2 t) \quad (2.2)$$

I: infiltration rate, [mm/h];
D: internal diameter of the infiltration opening, [mm];
M: mass of infiltrated water, [kg];
t: measured time required to infiltrate the measured amount of water into the pavement [s].
γ: unit-conversion constant, 4,583,666,000 for M in kg, D in mm and t in seconds [33].

The values in Table 5 are expressed in cm/s, using 1 cm/s = 36,000 mm/h. Equation (2) gives an average surface infiltration rate under the test conditions, not a Darcy permeability coefficient. ASTM C1701 is cited for the calculation; the finite-volume laboratory arrangement is not claimed to reproduce the complete in-place standard procedure. Comparisons with other hydraulic methods require consideration of their different test conditions [34].

Infiltration is a critical parameter for both stormwater management and thermal performance, as it affects water entry and redistribution within the pavement system [28].

2.5. Thermal conductivity

Thermal conductivity measurements were conducted using the hot-wire method on 15 × 15 × 6 cm³ specimens, as described in earlier pervious-concrete work [8]. This technique allows the evaluation of the effective thermo-physical properties of pervious concrete, which influence heat transfer through the pavement layer.

Previous studies have shown that thermal conductivity is strongly affected by porosity, aggregate type and moisture content, and plays a significant role in the surface energy balance of pavements [8].

2.6. Experimental setup for thermal behaviour

2.6.1. Bench and instrumentation

The bench developed for earlier pervious-pavement studies [8] comprised an acrylic tank with two 20 × 30 × 15 cm³ compartments. The central separator could be removed to accommodate one 30 × 40 cm slab; this full-width configuration was used here. A 10 cm layer of sand graded 0.08–5 mm was placed below the 5 cm paver to represent the underlying reservoir layer. The sidewalls were insulated with mineral wool (nominal thermal conductivity 0.03 $W \cdot m^{-1} \cdot K^{-1}$), and lateral gaps were sealed during wet tests to limit evaporation outside the exposed upper surface.

Radiative forcing was supplied by two 1000 W infrared lamps with a principal wavelength of 1180 nm. Lamp height was adjustable from 30 to 44 cm, and a power controller allowed repeatable irradiance. Surface temperature at the centre of the slab was measured with an optical infrared sensor having a distance-to-spot ratio of 15:1. Thermocouples were available at nominal depths of 0, 2.35, 6.90 and 10.00 cm, with additional sensors at the paver–base interface and tank bottom. A CMP3 pyranometer (300–2800 nm) measured shortwave flux, a CGR3 pyrgeometer (4500–42,000 nm) measured longwave flux, and an ALMEMO 2890-9 system recorded the sensor outputs. The complete bench and the test configuration are shown in Fig. 5.



Fig. 5. The experimental setup

2.6.2. Dry and wet protocols

The bench was operated in a controlled room at 20–23 °C and 35–40% relative humidity. The incident shortwave irradiance during lamp-on periods was 520 $W \cdot m^{-2}$, and all channels were recorded every 2

min. One slab per formulation was tested sequentially under the same programmed forcing. The terms "lamp-on" and "lamp-off" denote laboratory daytime heating and nighttime cooling, respectively. Table 3 summarizes the test protocol.

Table 3. Controlled thermal-test protocol

Condition	Initial state	Duration	Cycle	Recorded outcomes
Dry	Oven-dried; cooled to room temperature	24 h	8 h lamp-on + 16 h lamp-off	Surface temperature
Wet	Water-saturated slab over initially dry sand; no subsequent water addition	120 h temperature; 96 h SPCP mass	Five cycles of 8 h lamp-on + 16 h lamp-off	Surface temperature, reflected shortwave flux, SPCP water mass

For the wet experiment, the slab was saturated with water at the start of the test and placed over initially dry sand, then followed for five consecutive 24 h cycles without further water addition. The SPCP mass record covers 96 h. The balance was zeroed with the dry slab and the other dry components in place; the recorded mass therefore represents water remaining in the weighed assembly, rather than total wet slab mass. This dry-baseline subtraction is consistent with the gravimetric approach in [35]. Water could redistribute between the slab and the underlying sand, so the record does not isolate water retained within the concrete alone. No corresponding CPCP mass record is available. Wet albedo was calculated only when the lamps were on. Values close to zero during lamp-off intervals reflect the absence of incident shortwave radiation and are not meaningful albedo measurements.

3. RESULTS

3.1. Aggregate characteristics

The seashell fraction differed from the natural aggregate in shape, grading, absorption and packing (Figs. 1 and 2; Table 1). Its loose bulk density was 760 kg·m^{-3}, 53.1% below the NA value, while its particle relative density was 2.860, 3.7% above the NA value of 2.757. The lower loose bulk density of SA must therefore not be attributed to a lower intrinsic particle density. It instead indicates inefficient bulk packing and a large interparticle void volume associated with the plate-like shell geometry and grading.

The 24 h water absorption of SA was 3.46%, approximately 6.3 times the NA value (0.55%). Because both mixes used the same nominal water content and the constituents were initially dry, this contrast could have reduced the water immediately available to the shell-mix paste and contributed to differences in coating and bond. The Los Angeles coefficient increased from 15% for NA to 23.84% for SA, indicating greater fragmentation under the specified test. XRD confirmed that the shells were dominated by aragonitic CaCO3 (Fig. 3). These characteristics provide plausible mechanisms for the observed concrete response, but the present experiment does not separate their individual effects. The 24 h absorption values do not establish the uptake during mixing or a measured effective water-to-cement ratio.

3.2. Physical and mechanical properties

Table 4 summarizes the physical and mechanical properties of the control pervious concrete pavers (CPCP) and the seashell-based pervious concrete pavers (SPCP), including bulk density, open porosity and 28-day compressive strength.

Replacing natural aggregates with seashell aggregates produced a clear lightweighting effect. The bulk density decreased from 1951 kg/m³ (CPCP) to 1584 kg/m³ (SPCP), i.e. a reduction of approximately 19%. This reduction is consistent with the lower bulk density of seashell aggregates compared to natural aggregates and reflects changes in packing efficiency and inter-particle voids, rather than a lower shell-particle density. In pervious concrete, density is a key driver of the mechanical–hydraulic balance: higher density typically enhances compressive strength but reduces porosity and permeability.

SPCP exhibited a substantially higher open porosity (37.7%) than CPCP (21.97%), corresponding to an increase of about 72%. This indicates a larger water-accessible void fraction in the shell-based formulation. Mechanistically, this behaviour may be associated with (i) the irregular morphology and surface roughness of seashell particles, which can reduce coating uniformity of the cement paste and increase inter-granular voids, and (ii) differences in aggregate grading and packing relative to the control mix. Importantly, pore structure should be interpreted beyond total void content, as connectivity and pore size distribution strongly influence functional performance.

As expected for pervious concrete, the increase in porosity in SPCP was accompanied by a decrease in compressive strength. At 28 days, compressive strength dropped from 11.6 MPa (CPCP) to 4.44 MPa (SPCP), i.e. a reduction of approximately 62%. This reflects the classical trade-off in pervious concrete: increasing the void ratio reduces the effective load-transfer area and can intensify stress concentrations within the paste–aggregate skeleton. In addition, seashell aggregates may contribute less mechanically than natural aggregates and can modify the paste microstructure and interfacial transition zone.

Seashell aggregates shift the material towards a more porous and lighter PCP, enhancing the pore network that governs hydrological and thermo-hydric functions while reducing compressive strength. This positioning is coherent with current research directions that emphasize performance balance (runoff reduction, cooling) alongside structural functionality, with further mechanical validation needed for the intended pavement application.

Table 4. Physical and mechanical properties of pavers. Values are means ± standard deviations for three specimens per formulation

Sample	Average open porosity (%)	Bulk density (kg/m³)	Compressive strength, 28 days (MPa)
CPCP	21.97 ± 1.67	1951 ± 42.33	11.6 ± 0.460
SPCP	37.7 ± 2.04	1584 ± 57.06	4.44 ± 0.396

3.3. Hydraulic and thermo-physical properties

The hydraulic and thermo-physical properties of CPCP and SPCP are reported in Table 5, including the measured infiltration rate (Eq. (2)) and key thermo-physical parameters (thermal conductivity and albedo). Overall, replacing natural aggregates with seashell aggregates shifts the material response toward a more hydro-active and thermally insulating pervious skeleton, which is particularly relevant for coupled stormwater–cooling performance.

SPCP exhibits a markedly higher infiltration rate than CPCP. The measured rate increases from 1.296 ± 0.051 cm/s (CPCP) to 3.07 ± 0.125 cm/s (SPCP), i.e. an increase of approximately +137%. This improvement is consistent with the higher open porosity of SPCP and is compatible with improved water access through the pore network [36]. Importantly, open porosity alone does not fully predict permeability; hydraulic conductivity also depends on pore connectivity, tortuosity, aggregate grading, paste coating thickness, and compaction.

From an application standpoint, the infiltration rate measured for SPCP is favourable for rapid infiltration and reduced surface water residence time. However, long-term hydraulic performance can be limited by clogging; therefore, the practical benefit of high initial infiltration depends on exposure conditions and maintenance strategies.

SPCP shows a substantial reduction in thermal conductivity compared to CPCP, decreasing from 0.613 ± 0.018 $W \cdot m^{-1} \cdot K^{-1}$ (CPCP) to 0.351 ± 0.022 $W \cdot m^{-1} \cdot K^{-1}$ (SPCP), i.e. approximately −43%. This reduction can be explained by (i) increased air-filled porosity, which reduces effective solid heat-transfer pathways, and (ii) aggregate-related effects that modify the continuity of the solid skeleton and paste–aggregate interfaces. Lower conductivity alters heat storage and release during heating/cooling cycles.

The measured dry-surface albedo of SPCP is slightly higher than that of CPCP, increasing from 0.203 ± 0.007 (CPCP) to 0.220 ± 0.005 (SPCP) ($\approx$ +8%). Although modest, this implies reduced shortwave absorption under identical radiative forcing. Wetting can reduce effective reflectance, which should be considered when interpreting wet-state temperature evolution.

Together, these results show that seashell aggregates generate a more permeable (water-accessible) and more insulating (lower conductivity) pavement, while slightly increasing dry albedo. This combination is favourable for wet-state cooling because higher infiltration and the open pore network can improve water access, but sustained cooling also depends on retention and near-surface water availability [37] (fueling evaporation), and lower conductivity limits conductive heat replenishment to the surface when evaporation is active. The implications of these coupled effects are examined through dry/wet surface temperature tests in Section 3.4.

Table 5. Paver infiltration rate, thermal conductivity, and albedo. Values are reported as means ± standard deviations; infiltration variability is based on three repeated measurements from one slab of each formulation

Sample	Infiltration rate (cm/s)	Thermal conductivity ($W \cdot m^{-1} \cdot K^{-1}$)	Albedo
CPCP	1.296 ± 0.051	0.613 ± 0.0176	0.203 ± 0.0073
SPCP	3.07 ± 0.125	0.351 ± 0.022	0.22 ± 0.0053

3.4. Thermal behaviour and surface temperature

3.4.1. Overview and interpretation framework (energy balance)

This section quantifies how replacing natural aggregates with recycled seashell aggregates modifies the thermal behaviour of pervious concrete pavers. CPCP and SPCP were tested under identical and repeatable radiative forcing in both dry and wet states. The surface response can be interpreted through a simplified surface energy balance in which (i) shortwave absorption is primarily controlled by albedo, (ii) sensible heat exchange depends on the air–surface temperature gradient, (iii) conduction and heat storage are governed by the effective thermal conductivity and the solid–void skeleton, and (iv) under wet conditions, latent heat extraction through evaporation can dominate the surface cooling response when moisture is available within the pore network.

In this framework, dry-state tests isolate radiative and conductive effects (albedo, conductivity, heat storage), whereas wet-state tests activate evaporative cooling and reveal the extent to which pore structure and hydraulic accessibility sustain evaporation and temperature depression.

3.4.2. Dry-state surface temperature response

Fig. 6 compares the surface temperature evolution of CPCP and SPCP under dry conditions. Because evaporation is negligible in the dry state, differences between CPCP and SPCP mainly reflect the influence of seashell aggregates on radiative and thermo-physical parameters. In this study, CPCP and SPCP reached almost the same maximum surface temperature during the heating phase (lamps on), while SPCP became cooler during the cooling phase (lamps off), with a maximum difference of approximately 5 °C.

This behaviour is consistent with the measured material properties. SPCP exhibits a slightly higher dry albedo than CPCP, which marginally reduces absorbed shortwave radiation. More importantly, SPCP shows a substantially lower thermal conductivity than CPCP. Lower conductivity limits conductive heat diffusion into deeper layers, altering heat storage and the timing of heat release. Under the same heating input, this can yield similar peak temperatures (when net radiation dominates), yet produce a cooler surface during the cooling period because the SPCP system stores and returns heat to the surface less efficiently [8].

The dry-state comparison therefore establishes a baseline: the seashell-based skeleton does not necessarily reduce peak temperature under strong heating, but it changes transient heat storage/release behaviour, which becomes crucial for interpreting the additional cooling contribution observed in wet conditions.

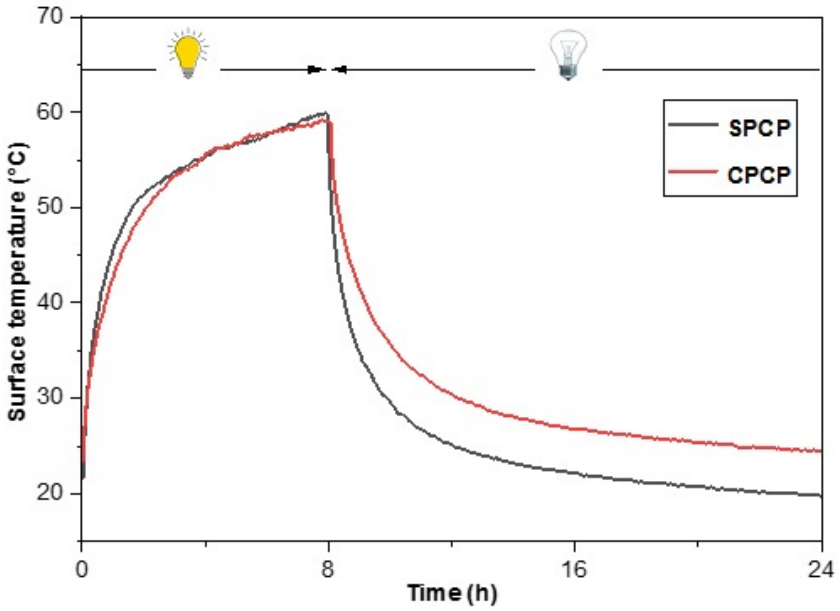

Fig. 6. Surface temperature evolution of CPCP and SPCP under dry conditions

3.4.3. Wet-state behaviour and evaporative cooling capacity

Under wet conditions (Fig. 7), both pavements exhibit lower surface temperatures than in the dry state, consistent with a contribution from latent heat extraction when water is available. SPCP shows enhanced

cooling relative to CPCP, with a reduction of up to about 7 °C during the heating phase (lamps on) and up to about 4 °C during the cooling phase (lamps off).

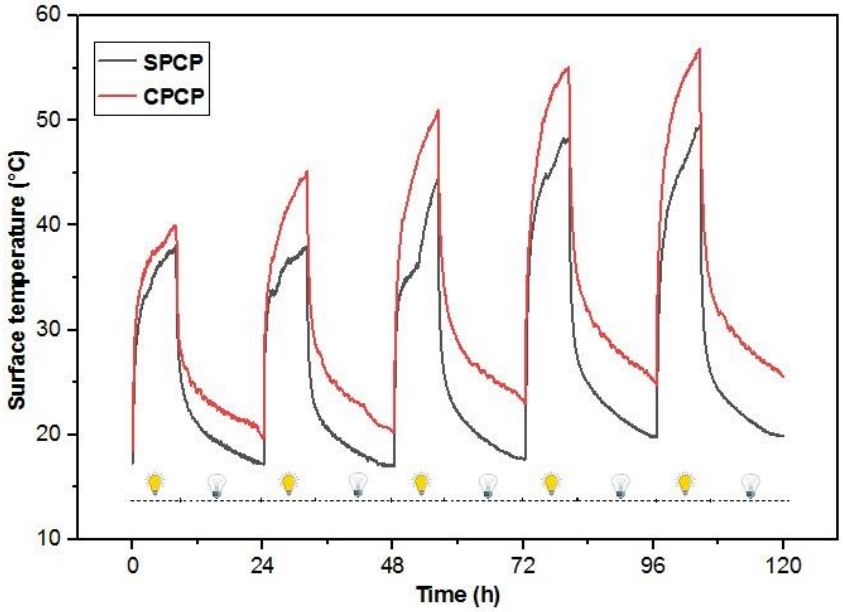

Fig. 7. Surface temperature variation of CPCP and SPCP under wet conditions

Mechanistically, the enhanced cooling of SPCP may be associated with the seashell-induced pore architecture and transport behaviour identified in Sections 3.1–3.3. The higher open porosity and infiltration rate of SPCP can improve moisture accessibility near the surface and support evaporation, while the lower thermal conductivity reduces conductive heat losses into underlying layers — both effects acting in concert to enhance the evaporative cooling response. However, recent research emphasizes that evaporative cooling depends on near-surface water availability rather than permeability alone [37,38], meaning that sustained cooling also requires adequate water retention within the pore network acting to amplify surface temperature depression when water is present.

This interpretation is supported by the mass evolution recorded during wet tests (SPCP weight change): the reduction in recorded water mass is consistent with evaporation during drying. The mass change shows that the water-loss rate of SPCP averaged 4.81 g/h in the first three days (see Fig. 8). The mass continued to decrease beyond 72 h and through the end of the 96 h record; the endpoint does not establish that evaporation had stopped.

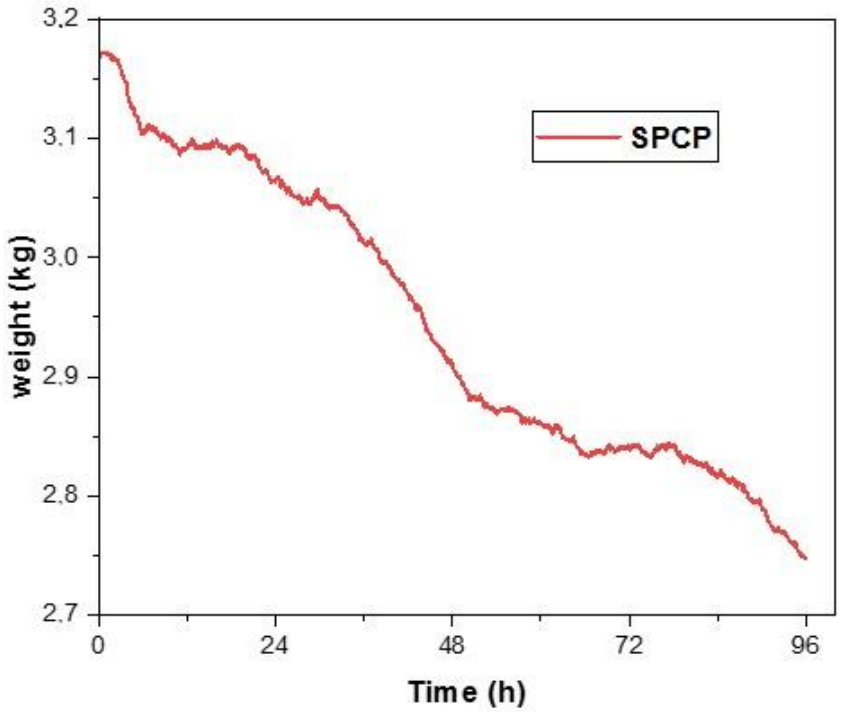

Fig. 8. SPCP weight change during wet test. The ordinate "weight (kg)" denotes water remaining after tare with the dry slab and other dry assembly components in place, not total slab mass or cumulative evaporated water

Wetting can reduce effective reflectance because water filling near-surface pores alters scattering/refraction and increases shortwave absorption. For SPCP, higher porosity and infiltration may influence this wet-optics shift if it helps maintain more moisture in near-surface pores. In practice, this may slightly disadvantage SPCP radiatively early in the wet heating period; however, in our results the net effect remains favourable, which is consistent with an evaporative contribution to cooling.

The albedo represents an additional factor influencing the surface temperature of SPCP. As shown in Fig. 9, on the third day the albedo of SPCP is still lower than that of CPCP, consistent with residual surface moisture (a wet surface presents a darker colour and therefore lower reflectance, as documented by Li et al. [39] and Mohegh et al. [40]). In the dry state, the slightly higher albedo of SPCP reduces shortwave absorption relative to CPCP. In the wet state, wetting lowers SPCP albedo below that of CPCP potentially through moisture redistribution within the pore network, which can sustain latent heat extraction; as a result, the net cooling effect remains favourable. Consistent with this interpretation, SPCP maintains lower surface temperatures than CPCP over the wet test period.

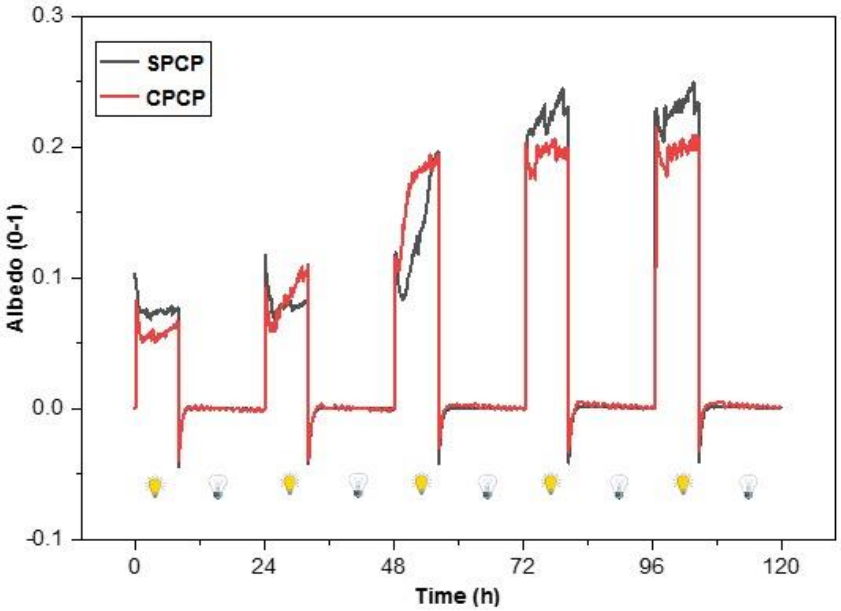

Fig. 9. Variation of pavement albedo under wet conditions

3.4.4. Coupling between pore structure, hydraulic properties and temperature evolution

Our results indicate that seashell aggregates modify the pervious concrete system in a direction that is favourable for hydro–thermal functionality, but with clear structural trade-offs.

Enhanced moisture access can support evaporation-driven cooling: the higher open porosity and measured infiltration rate of SPCP facilitate rapid infiltration and promote the presence of water within the near-surface pore network, which is the essential reservoir for evaporative cooling. Lower thermal conductivity further supports cooling persistence by limiting conductive heat replenishment of the surface when evaporation is active.

The main limitation is the strength reduction associated with a higher void network and a modified aggregate skeleton, which limits potential load-bearing applications unless optimization and further mechanical validation are undertaken. In addition, despite higher initial infiltration, fine sediments can still reduce infiltration over time; therefore, the long-term benefit depends on site conditions (sediment loads) and maintenance regime.

4. DISCUSSION

4.1. Comparison with previous studies

Nguyen et al. [15] obtained compressive strengths of 16 MPa for control pavers and 15 MPa for pavers incorporating seashells at partial replacement levels. The present values, 11.6 MPa for CPCP and 4.44 MPa for SPCP, show a larger strength penalty for the selected full-replacement formulation. Their reported permeability range of 3–8 mm/s is numerically below the present infiltration rates of 12.96 and 30.7 mm/s. However, differences in replacement level, grading, compaction and hydraulic test conditions prevent a direct ranking. The present results therefore represent a particular balance between drainage and strength, not an inevitable response of all shell-based concretes.

The CPCP reference and its reported characterization values are the same baseline used in the earlier study by Seifeddine et al. [8]. Agreement with those values is therefore not independent validation. The contribution here is the comparison with SPCP and the combined assessment of hydraulic, mechanical and dry–wet thermal responses.

For cooling, Qin et al. [28] reported water-retaining pavers with surface temperatures 2–10 °C below conventional or pervious comparison blocks. The maximum wet lamp-on difference of about 7 °C observed here is of the same order. It is not an unprecedented cooling magnitude, and differences in moisture storage, reference material and thermal forcing preclude direct performance ranking. The SPCP mass record supports continued drying beyond three days.

4.2. Circular-economy and cost considerations

The circular-economy contribution is the recovery of an available seashell resource to replace virgin coarse aggregate. For the present material, obtained from seashell accumulations through a local supplier, this does not demonstrate diversion of fresh seafood-processing waste. Economic feasibility depends on the delivered seashell price and the costs of washing, drying, screening, handling and transport. Both mixtures contain 350 kg/m³ of cement, so no cement-cost saving was achieved. The lower strength may also affect pavement thickness, support requirements and service life. Since a cost inventory and life-cycle assessment were not undertaken, the hydraulic and cooling gains cannot yet be translated into a claim of lower overall cost or environmental impact.

4.3. Future theoretical investigation

The temperature curves in Figs. 6 and 7 could be investigated further with a transient energy equation accounting for conduction and heat storage in the slab and sand, absorbed radiation, longwave emission and convection. The energy-equation approaches applied to underground ice-ring evolution [41] and moving solid-fuel heating [42] illustrate how thermal responses can be analysed theoretically, although their boundary conditions and physical processes differ from those of pavements. A pavement model could first be tested against the dry-state measurements, then extended to moisture redistribution and latent heat extraction under wet conditions, including the initially dry base layer. Independently measured thermal and moisture parameters and repeated temperature and water-loss records would be needed for validation. Such modelling remains future work; the present interpretation is not a theoretical validation of the measured curves.

5. CONCLUSIONS

This study assessed the effect of recycled seashell aggregates on the physical, mechanical, hydraulic, and thermo-physical performance of pervious concrete pavers, with a specific focus on surface thermal behaviour under dry and wet conditions. Control pervious concrete pavers (CPCP) were compared with seashell-based pervious concrete pavers (SPCP). The main conclusions are:

SPCP exhibited a 72% increase in open porosity compared to CPCP and a lower bulk density, reaching 1584 kg/m³, confirming the lightweighting effect of seashell aggregates.

SPCP exhibited a higher measured infiltration rate, with an increase of about 137% compared to CPCP, demonstrating the clear advantage of seashell aggregates for stormwater infiltration and rapid drainage.

The 28-day compressive strength of SPCP was 4.44 MPa, a 62% reduction from CPCP (11.6 MPa), corresponding to approximately 38% of the CPCP strength. This confirms the classical pervious-concrete trade-off: improving hydraulic functionality by increasing pore volume/connectivity reduces

load-bearing capacity; suitability for any traffic class requires further mechanical and durability validation.

SPCP presented a 43% lower thermal conductivity than CPCP, which influences transient heat storage and release. Under dry conditions, CPCP and SPCP reached nearly the same maximum surface temperature during the heating stage (lamps on), but SPCP showed a cooler surface during the cooling stage (lamps off), with a maximum difference of about 5 °C.

Under wet conditions, SPCP achieved stronger surface cooling than CPCP, with temperature reductions reaching up to 7 °C during heating (lamps on) and up to 4 °C during cooling (lamps off).

Seashell aggregates shift pervious concrete pavers toward a highly permeable, thermally insulating and wet-cooling-efficient material. This makes SPCP a promising solution for stormwater volume management and urban heat island mitigation, particularly in contexts where pavements are periodically wetted (rain events or watering strategies). The main limitation remains the reduced mechanical strength associated with the high-void skeleton.

Outlook / recommended next steps

To better balance structural and functional performance, future research should focus on optimizing the SPCP mix design, for example by incorporating controlled amounts of seashell sand or adjusting aggregate grading and compaction in order to reduce excessive porosity while preserving permeability. Further work is also needed to assess durability and clogging sensitivity under representative sediment exposure and maintenance protocols. Finally, field-scale validation under real weather conditions and seasonal climatic cycles is necessary to confirm the long-term cooling potential and practical applicability of seashell-based pervious concrete pavers.

Study limitations

Although the present results clearly demonstrate the potential of SPCP for improving infiltration and wet-state cooling, several limitations should be acknowledged before field implementation. The wet-state cooling results were obtained under controlled laboratory conditions with a fixed radiative regime and initial saturation without subsequent water addition; field performance under natural rainfall, variable solar loading, clogging, drying cycles, and traffic wear may differ and should be validated through outdoor monitoring. First, the long-term hydraulic behaviour of SPCP under clogging conditions was not investigated, even though clogging is a key factor governing the in-service performance of pervious concrete pavements. Second, durability-related aspects such as abrasion resistance, freeze–thaw behaviour, and long-term environmental exposure were beyond the scope of this study. The comparison is limited to two formulations and cannot isolate mineralogy, grading, packing and absorption effects or identify an optimum shell content. One thermal slab per formulation and repeated infiltration measurements on one slab limit the assessment of specimen-to-specimen variability. Future comparisons should control grading and aggregate moisture and include absorption kinetics beyond 24 h.

ADDITIONAL INFORMATION

Disclosure statement: No potential conflict of interest was reported by the authors.

REFERENCES

1. Imroz, M, Akhtar, MP, Sharma, MK and Alshehri, F 2025. Integrated assessment of urban flooding and heat island interactions: A systematic review of geospatial technologies, machine learning approaches, and microclimate dynamics. J. Environ. Manage. 395, 127984.
2. Seifeddine, K, Amziane, S and Toussaint, E 2022. State of the art on the mechanical properties of pervious concrete. Eur. J. Environ. Civ. Eng. 26(15), 7727-7755.
3. Adresi, M, Yamani, AR and Tabarestani, MK 2024. Evaluating the effectiveness of innovative pervious concrete pavement system for mitigating urban heat island effects, de-icing, and de-clogging. Constr. Build. Mater. 449, 138361.
4. Akkaya, A and Çağatay, İH 2021. Investigation of the density, porosity, and permeability properties of pervious concrete with different methods. Constr. Build. Mater. 294, 123539.
5. AlShareedah, O and Nassiri, S 2021. Spherical discrete element model for estimating the hydraulic conductivity and pore clogging of pervious concrete. Constr. Build. Mater. 305, 124749.
6. Chen, L-M, Chen, J-W, Lecher, T and Davidson, PC 2025. A field-scale assessment of the impact of conventional and permeable concrete pavements on surface and air temperatures. Environments 12(6), 192.
7. Torres-Molina, L 2025. Pervious concrete for urban heat island. Proceedings of the LACCEI International Multi-Conference for Engineering, Education and Technology.
8. Seifeddine, K, Amziane, S and Toussaint, E 2022. Thermal behavior of pervious concrete in dry conditions. Constr. Build. Mater. 345, 128300.
9. Shakrani, SA, Ayob, A and Rahim, MAA 2017. Applications of waste material in the pervious concrete pavement: A review. AIP Conf. Proc. 1885.
10. Vijayalakshmi, R 2021. Recent Studies on the Properties of Pervious Concrete; A Sustainable Solution for Pavements and Water Treatment. Civil and Environmental Engineering Reports 31(3), 54–84. https://doi.org/10.2478/ceer-2021-0034.
11. Hwang, SS and Cortés, CMM 2021. Properties of mortar and pervious concrete with co-utilization of coal fly ash and waste glass powder as partial cement replacements. Constr. Build. Mater. 270.
12. Hamada, HM, Al-Attar, A, Askar, MK, Beddu, S, Majdi, A and Humada, AM 2025. Recycled seashells as sustainable aggregates in concrete: Advancing waste management and enhancing performance: A comprehensive review. Journal of Building Engineering 110(2), 113067.
13. Tayeh, BA and others 2020. Durability and mechanical properties of seashell partially-replaced cement. Journal of Building Engineering 31.
14. Nguyen, DH, Boutouil, M, Sebaibi, N, Baraud, F and Leleyter, L 2017. Durability of pervious concrete using crushed seashells. Constr. Build. Mater. 135(2017), 137-150.
15. Nguyen, DH, Boutouil, M, Sebaibi, N, Leleyter, L and Baraud, F 2013. Valorization of seashell by-products in pervious concrete pavers. Constr. Build. Mater. 49, 151-160.
16. Eziefula, UG, Ezeh, JC and Eziefula, BI 2018. Properties of seashell aggregate concrete: A review. Constr. Build. Mater. 192, 287-300.
17. Zhu, Y, Chen, D, Yu, X, Liu, R and Liao, Y 2024. Properties of Cementitious Materials Utilizing Seashells as Aggregate or Cement: Prospects and Challenges. Materials.
18. Castañeda, D, Varhen, C, Guerrero, RFE and Ruiz, G 2025. Enhancing pervious concrete performance using industrial waste: a study on crushed scallop seashell waste (CSS) and recycled cellulose fibre (CF). Construction and Building Materials.
19. de Freitas, JJG, Vieira, CMF, Natalli, JF, Lavander, HD and de Azevedo, ARG 2024. Cleaner production of cementitious materials containing bioaggregates based on mussel shells: a review. Sustainability 16(13), 5577.

20. Essalem, MLM, Cherradi, T, Amziane, S and Teguedy, MC 2023. Influence of Seashell on the Physical, Mechanical and Thermal Properties of Brick Mortar Mixtures. The Open Civil Engineering Journal 17(1), 1-8.
21. Horiguchi, I, Mimura, Y and Monteiro, PJM 2021. Plant-growing performance of pervious concrete containing crushed oyster shell aggregate. Clean. Mater. 2, 100027.
22. Gonzalez-Caro, A, Lamaa, G, Silva, RV, de Brito, J and Jiménez, JR 2025. CO2-cured alkali-activated pervious paving blocks incorporating seashell sand. Materials and Structures.
23. Essalem, MLM and Cherradi, T 2023. Seashell as Aggregate in Cemented Materials: A Review. Civil Engineering and Architecture 11(3), 1337-1345.
24. Eo, S and Yi, S 2015. Effect of oyster shell as an aggregate replacement on the characteristics of concrete. Magazine of Concrete Research 67(15).
25. ASTM 2015. ASTM C127-15. Standard Test Method for Relative Density (Specific Gravity) and Absorption of Coarse Aggregate.
26. ASTM 2023. ASTM C29/C29M. Standard Test Method for Bulk Density (Unit Weight) and Voids in Aggregate.
27. Qin, Y 2015. A review on the development of cool pavements to mitigate urban heat island effect. Renewable and sustainable energy reviews 52, 445-459.
28. Qin, Y, He, Y, Hiller, JE and Mei, G 2018. A new water-retaining paver block for reducing runoff and cooling pavement. J. Clean. Prod. 199, 948-956.
29. Haselbach, L, Boyer, M, Kevern, JT and Schaefer, VR 2011. Cyclic heat island impacts on traditional versus pervious concrete pavement systems. Transp. Res. Rec. 2240(1), 107-115.
30. Neithalath, N, Weiss, J and Olek, J 2006. Characterizing enhanced porosity concrete using electrical impedance to predict acoustic and hydraulic performance. Cem. Concr. Res. 36(11), 2074-2085.
31. Neithalath, N, Sumanasooriya, MS and Deo, O 2010. Characterizing pore volume, sizes, and connectivity in pervious concretes for permeability prediction. Mater. Charact. 61(8), 802-813.
32. Qin, Y and Hiller, JE 2016. Water availability near the surface dominates the evaporation of pervious concrete. Constr. Build. Mater. 111, 77-84.
33. ASTM. ASTM C1701/C1701M. Standard Test Method for Infiltration Rate of In Place Pervious Concrete.
34. Li, H, Kayhanian, M and Harvey, JT 2013. Comparative field permeability measurement of permeable pavements using ASTM C1701 and NCAT permeameter methods. J. Environ. Manage. 118, 144-152.
35. Seifeddine, K, Amziane, S and Toussaint, E 2022. Experimental investigation of physical characteristics to improve the cooling effect of permeable pavements. Construction and Building Materials 345, 128342. https://doi.org/10.1016/j.conbuildmat.2022.128342.
36. Shan, J and others 2022. Pore characteristics of pervious concrete and their influence on permeability attributes. Constr. Build. Mater. 327, 126874.
37. Starke, P, Göbel, P and Coldewey, WG 2010. Urban evaporation rates for water-permeable pavements. Water Sci. Technol. 62(5), 1161-1169.
38. Syrrakou, C and Pinder, GF 2014. Experimentally determined evaporation rates in pervious concrete systems. J. Irrig. Drain. Eng. 140(1), 04013003.
39. Li, H, Harvey, J and Kendall, A 2013. Field measurement of albedo for different land cover materials and effects on thermal performance. Build. Environ. 59, 536-546.
40. Mohegh, A, Rosado, P, Jin, L, Millstein, D and Levinson, R 2017. Modeling the climate impacts of deploying solar reflective cool pavements in California cities. J. Geophys. Res. Atmos. 122(6798), 6798-6817.

41. Turkyilmazoglu, M and Alotaibi, A 2026. Prolonging the life time of underground ice ring formed in the period of the cryogenic gas storage. European Journal of Mechanics B Fluids 115, 204395. https://doi.org/10.1016/j.euromechflu.2025.204395.
42. Turkyilmazoglu, M 2020. Combustion of a solid fuel material at motion. Energy 203, 117837. https://doi.org/10.1016/j.energy.2020.117837.